ACS OMEGA

http://pubs.acs.org/journal/acsodf

Article

Adsorption Behavior of Environmental Gas Molecules on Pristine and Defective $MoSi_2N_4$: Possible Application as Highly Sensitive and Reusable Gas Sensors

Chengwei Xiao, Zuju Ma,* Rongjian Sa, Zhitao Cui, Shuaishuai Gao, Wei Du, Xueqin Sun, and Qiao-hong Li

Cite This: *ACS Omega* 2022, 7, 8706−8716

Read Online

ACCESS | Metrics & More | Article Recommendations | Supporting Information

ABSTRACT: Inspired by the recent practical application of two-dimensional (2D) nanomaterials as gas sensors, catalysts, and materials for waste gas disposal, herein, the adsorption behaviors of environmental gas molecules, including NO, CO, O_2, CO_2, NO_2, H_2O, H_2S, and NH_3, on the 2D pristine and defective $MoSi_2N_4$ (MSN) monolayers were systematically investigated using spin-polarized density functional theory (DFT) calculations. Our results reveal that all the gas molecules are physically adsorbed on the MSN surface with small charge transfer, but the electronic structures of NO, NO_2, and O_2 are obviously modified due to the in-gap states. The introduction of N vacancy on the MSN surface enhances the interaction between gas molecules and the substrate, especially for NO_2 and O_2. Interestingly, the adsorption type of NO and CO evolves from physisorption to chemisorption, which may be utilized in NO and CO catalytic reaction. Furthermore, the moderate adsorption strength and obvious changes in electronic properties of H_2O and H_2S on the defective MSN make them have promising prospects in highly sensitive and reusable gas sensors. This work offers several promising gas sensors based on the MSN monolayer and also provides a theoretical reference of other related 2D materials in the field of gas sensors, catalysts, and toxic gas disposal.

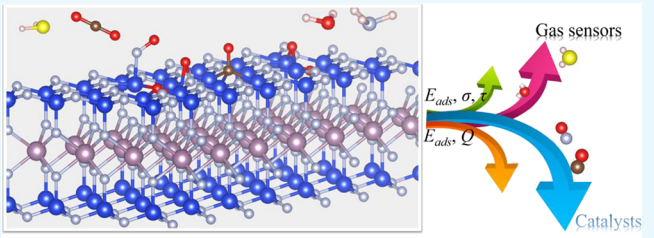

1. INTRODUCTION

Followed by the successful isolation of graphene,[1,2] an upsurge in the study of two-dimensional (2D) materials has started, such as silicene,[3−6] phosphorene,[7,8] and transition metal dichalcogenides.[9−13] Due to the quantum size effect, the 2D materials holding a high surface-to-volume ratio have fascinating physicochemical and electronic properties.[14−16] These unique natures endow them with widespread application prospects, including energy conversion or storage,[17,18] photo/electrocatalysis,[19−22] nanoelectronics,[23,24] and gas sensing.[25−27] The development of new 2D materials has not stagnated either experimentally or theoretically. Very recently, a new series of 2D van der Waals (vdW) layered materials named MA_2Z_4 with a septuple-atomic-layer structure (M signifies a transition metal, *e.g.*, W, V, Nb, Ta, Ti, Zr, Hf, or Cr; A represents Si or Ge; Z stands for N, P, or As) have been predicted theoretically through DFT calculations.[28] Among them, the $MoSi_2N_4$ (MSN) monolayer was even synthesized successfully via chemical vapor deposition (CVD) with a Cu/Mo bilayer as the substrate and NH_3 gas as the nitrogen source.[28] Both the experiments and theoretical calculations show that the MSN monolayer exhibits outstanding ambient stability and behaves as an indirect semiconductor.[28,29] In addition, it was found that the hole and electron mobilities of the monolayer MSN[28] are about 4−6 times greater than that of the monolayer MoS_2.[30] These fascinating properties render the monolayer MSN promising potential in the application of nanoelectronics and optoelectronics. Recently, the electrical contact physics properties of the MSN monolayer were investigated and the ultralow Schottky barrier height of $MoSi_2N_4/NbS_2$ contact was exhibited, which demonstrates its application prospect in the nanoelectronic devices.[31] The tunable electronic structures and piezoelectric coefficients by strain make the monolayer MSN beneficial to the fabrication of nanodevices.[32] In addition, previous work also revealed that the MSN monolayer possesses potential application in the field of photocatalysis owing to the suitable band gap and band edge positions.[29]

The detection of specific small gas molecules, such as NO, CO, O_2, CO_2, NO_2, H_2O, H_2S, and NH_3, is of great significance for public safety, environmental protection, industrial manufacture, and medical diagnosis. 2D materials

Received: December 4, 2021
Accepted: February 11, 2022
Published: February 28, 2022

https://doi.org/10.1021/acsomega.1c06860
ACS Omega 2022, 7, 8706−8716

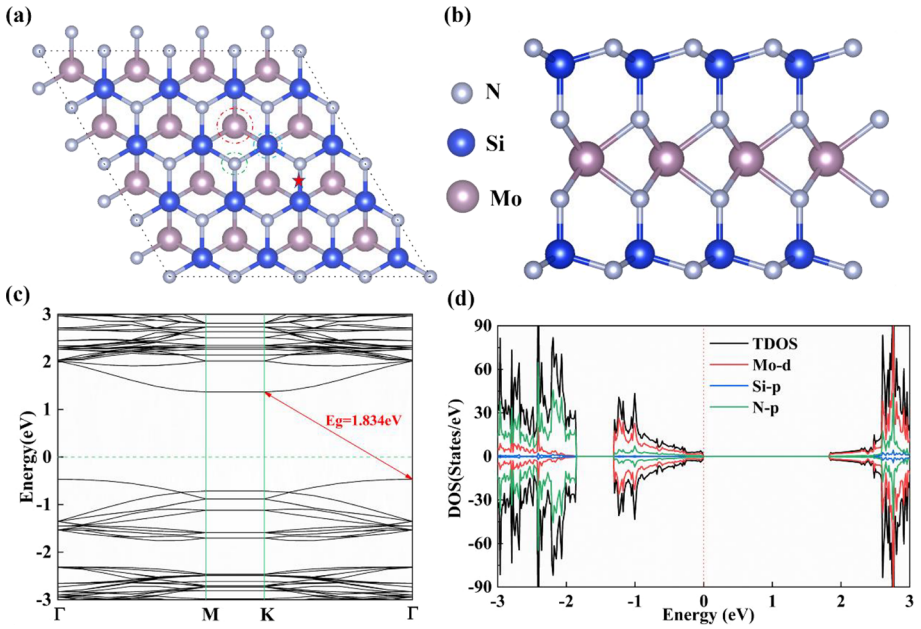

Figure 1. (a) Top and (b) side views of the optimized MSN monolayer and the calculated (c) band structure and (d) DOS of the pristine MSN monolayer. The considered possible adsorption sites for gas molecules are shown in panel (a). The Fermi level is set to zero.

gain enormous attention for gas sensors due to the high surface-to-volume ratio, exposure of active sites, and high carrier mobility.[11,13,33,34] However, as we all know, there exist many small gas molecules on the surface of 2D materials, and it is impossible to completely remove them due to the large surface area.[35,36] Interestingly, previous reports show that even the physisorption of small gas molecules also has an effective influence on the electronic and optical properties of 2D materials, which is vital for developing a high-performance gas sensor.[37−39] Over the past two decades, the adsorption behaviors of gas molecules on a train of 2D nanomaterials, including graphene,[25,40,41] stanene,[42,43] blue phosphorus,[44] InSe,[34,45] and MoS_2 monolayer,[13,46,47] have been investigated in detail and the graphene-based gas sensors have already been used in practice.[48] Earlier this year, Bafekry et al.[49] investigated the adsorption behavior of environmental gas molecules on the pristine MSN monolayer and found that the magnetic properties of MSN were changed by adsorption of O_2, NO, and NO_2; however, the application of gas sensors based on pristine MSN is severely restricted due to the weak interaction and few charge transfer.

In this study, we performed a systemic theoretical study on the adsorption behavior of gas molecules (NO, CO, O_2, CO_2, NO_2, H_2O, H_2S, and NH_3) on MSN and N-defective MSN (d-MSN) monolayers, concentrating on the most stable adsorption configurations, charge transfer and the changes of electronic structures and properties, and possible applications. We found that all the gas molecules are physisorbed on pristine MSN with a little charge transfer. However, the introduction of N vacancy on the MSN surface enhances the interaction between gas molecules and MSN, and the adsorption type of CO and NO changes from physisorption to chemisorption. Furthermore, the d-MSN has moderate adsorption strength on H_2O and H_2S, which endows them with bright application prospects in H_2O and H_2S gas sensors.

2. COMPUTATIONAL METHODS

All the DFT calculations were performed as implemented in the Vienna Ab-initio Simulation Package (VASP).[50,51] The ion−electron interaction and exchange-correlation functional were treated by the projected augment wave (PAW) pseudopotentials[52] and Perdew−Burke−Ernzerhof (PBE) version of the generalized gradient approximation (GGA),[53] respectively. The valence electronic configurations of Mo, Si, N, C, O, S, and H are $4p^6 5s^2 4d^4$, $3s^2 3p^2$, $2s^2 2p^3$, $2s^2 2p^2$, $2s^2 2p^4$, $3s^2 3p^4$, and $1s^1$, respectively. A vacuum region of 15 Å in the z direction was employed to eliminate the interaction between the periodic layers. The energy cutoff of 500 eV was adopted for plane wave expansion. The gamma-centered $3 \times 3 \times 1$ and $5 \times 5 \times 1$ k-point meshes in the Monkhorst−Pack scheme for the Brillouin zone sampling were used for the geometric optimization and electronic structure calculations of a $4 \times 4 \times 1$ supercell, respectively. The thresholds of energy and force were set to 0.02 eV/Å and 1.0×10^{-5} eV/atom, respectively. The vdW interaction was corrected by utilizing Grimme's scheme (D3)[54] and spin-polarization was considered in the whole calculations.

The stability of gas molecule adsorption on the MSN monolayer was estimated by the adsorption energy (E_{ads}), which is defined as:

$$E_{ads} = E_{gas-MSN} - E_{MSN} - E_{gas} \quad (1)$$

where $E_{gas-MSN}$, E_{MSN}, and E_{gas} denote the self-consistent energies of the MSN adsorbing different gas molecules, the pure MSN monolayer, and the free gas molecules. Based on the above equation, the negative value of the adsorption energy illustrates that the adsorption process is exothermic and the adsorption configuration is thermodynamically favorable.[55,56] To better elucidate the electronic interaction and visualize the charge transfer between the gas molecules and the MSN monolayer, the charge density difference (CDD) is defined as the following equation:

$$\Delta\rho = \rho_{gas-MSN} - \rho_{MSN} - \rho_{gas} \quad (2)$$

https://doi.org/10.1021/acsomega.1c06860
ACS Omega 2022, 7, 8706−8716

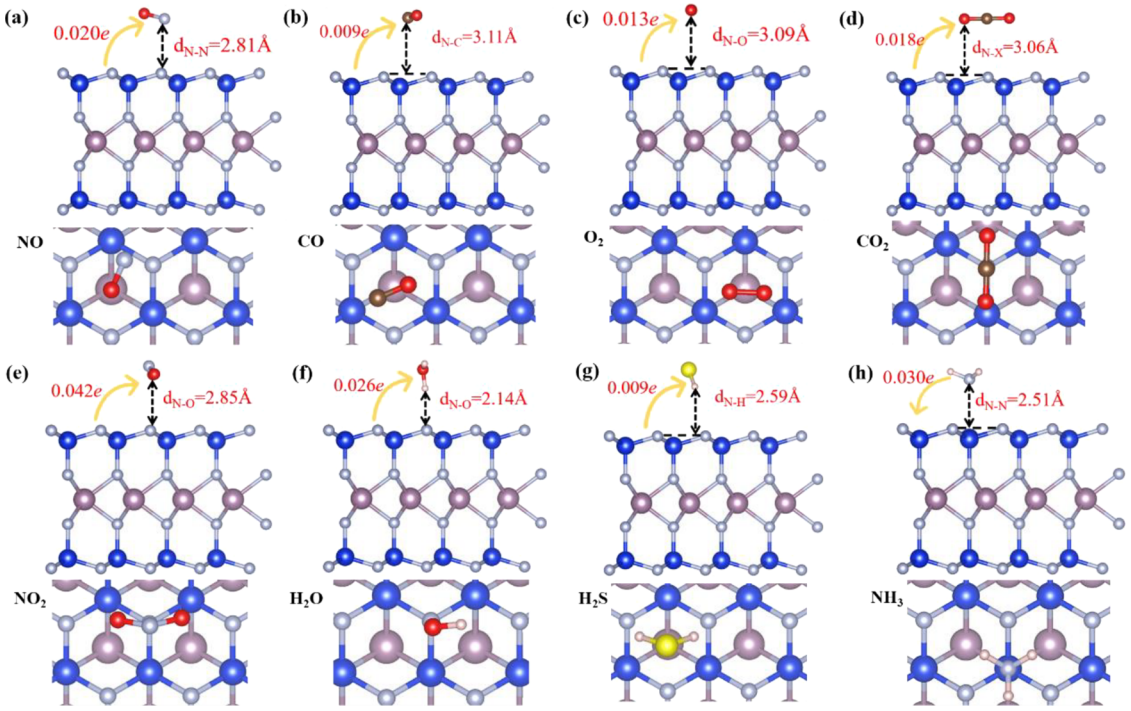

Figure 2. Top and side views of the most stable adsorption configurations of MSN adsorbing (a) NO, (b) CO, (c) O_2, (d) CO_2, (e) NO_2, (f) H_2O, (g) H_2S, and (h) NH_3.

where $\rho_{gas-MSN}$, ρ_{MSN}, and ρ_{gas} are the total charge densities of the gas molecules adsorbed by the MSN monolayer, those by the pure MSN monolayer, and the free gas molecules, respectively. The CDD plots are drawn by VESTA.[57]

3. RESULTS AND DISCUSSION

3.1. The Geometry and Electronic Structure of the MSN Monolayer. The MSN monolayer can be regarded as a 2H-MoS_2-like MoN_2 layer sandwiched by two InSe-like N−Si bilayers, forming a 2D honeycomb lattice with a space group of $P\bar{6}m2$ (no. 187) (see Figure 1a,b). The calculated lattice constants ($a = b = 2.90$ Å), bond lengths ($d_{N-Si} = 1.74-1.75$ Å and $d_{N-Mo} = 2.09$ Å), and the thickness (7.01 Å) of the MSN monolayer are in good agreement with previous work.[29] The calculated band structure and density of states (DOS) of the MSN monolayer are illustrated in Figure 1c,d. It is clearly observed that the MSN monolayer is an indirect semiconductor with the valence band maximum (VBM) located at the Γ point (0 0 0) and the conduction band minimum (CBM) at the *K* point (0.333 0.333 0). The obtained band gap is 1.83 eV, which is in good consistency with a previous experimental result of 1.94 eV[28] and a theoretical value of 1.79 eV.[29] The band gap calculated by the HSE06 method is 2.35 eV,[58−60] which overestimates the experimental data. Therefore, it suggests that the PBE functional can well describe the electronic structure of the MSN monolayer. Both the CBM and VBM of the pristine MSN monolayer are mainly contributed by Mo 4d orbitals, N 2p orbitals, and their hybridizations. Meanwhile, in the deeper region of the valence band, the N 2p states make the main contribution.

3.2. Adsorption Configurations and Adsorption Energies. To obtain the most stable adsorption site for different gas molecules, four possible adsorption sites are considered, including the top site of a N atom or Si atom, the bridge site of a N−Si bond, and the center of a N_3Si_3 hexagon ring, as illustrated in Figure 1a. In each site, the gas molecules were placed in end-on and side-on ways, respectively. Moreover, the initial adsorption configurations are different for the linear molecules (NO, CO, O_2, and CO_2) and the nonlinear molecules (NO_2, H_2O, H_2S, and NH_3). The details can be found in Figures S1−S3. The free gas molecules are optimized and displayed in Figure S4 with the bond lengths and angles being consistent with previous results.[13,42,45] After full optimization of the adsorption models, the most stable adsorption configurations of each molecule and corresponding adsorption energies (E_{ads}) are shown in Figures 2 and 3,

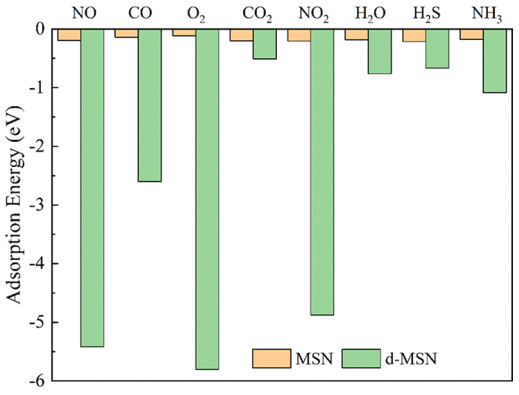

Figure 3. E_{ads} of NO, CO, O_2, CO_2, NO_2, H_2O, H_2S, and NH_3 on pristine MSN and d-MSN monolayers.

respectively. The E_{ads} values of other metastable adsorption structures are listed in Table S1. From Figure 2, we see that all the molecules tend to be adsorbed in a parallel manner to the MSN surface, except H_2O, which adopts a vertical alignment with the MSN surface. It is observed that most linear molecules (NO, CO, and O_2) and H_2S tend to be adsorbed

https://doi.org/10.1021/acsomega.1c06860
ACS Omega 2022, 7, 8706−8716

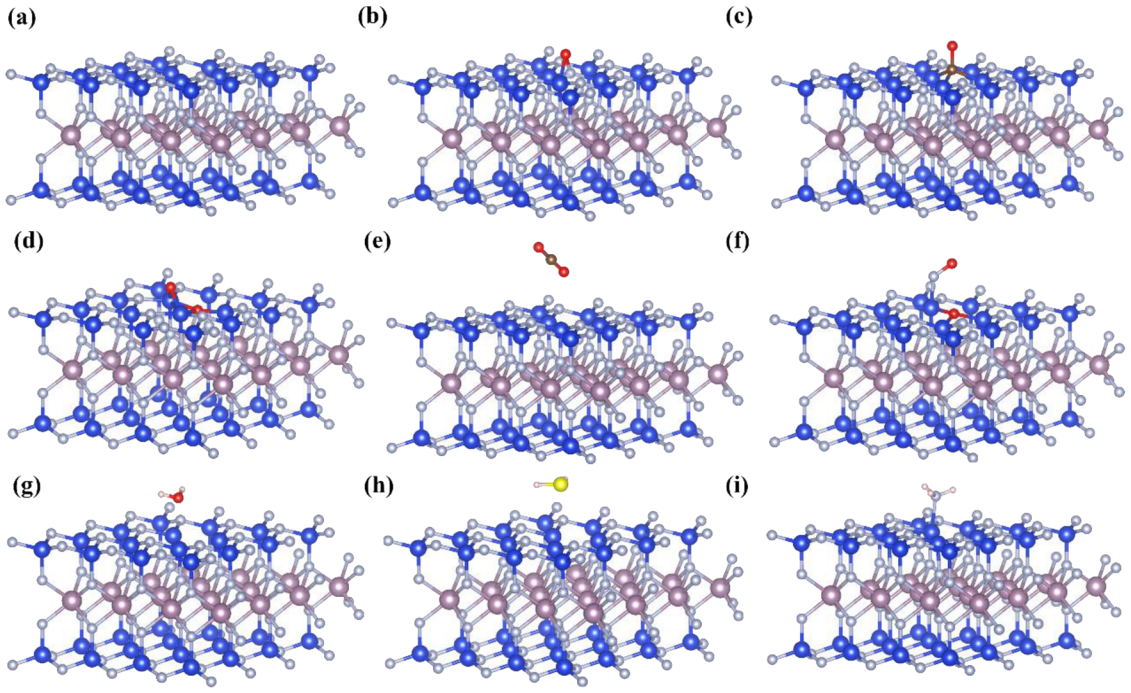

Figure 4. Optimized structure of (a) d-MSN and the most stable adsorption configurations of d-MSN adsorbing (b) NO, (c) CO, (d) O_2, (e) CO_2, (f) NO_2, (g) H_2O, (h) H_2S, and (i) NH_3.

above the center of the Ni_3Si_3 hexagon ring, while NO_2, CO_2, and H_2O locate on the top site of the N atom. The obtained E_{ads} values are all negative, indicating that adsorption processes for these molecules are thermodynamically favorable. The adsorption strength of the gas molecules on the MSN surface increases in the following order: O_2 < CO < NH_3 < H_2O < NO < CO_2 < NO_2 < H_2S. The results show that the adsorption strength of H_2S, NO_2, and CO_2 on the MSN monolayer stands out in the above gas molecules. Ma et al.[45] reported that the E_{ads} of NO_2 on the InSe monolayer is −0.21 eV and they supposed that the InSe monolayer has great promise for NO_2 sensing due to its higher electron mobility. In addition, Yu et al.[56] systematically investigated the adsorption behavior of various gas molecules on the Ti_2CO_2 monolayer and found that only NH_3 can be chemisorbed on Ti_2CO_2 with the E_{ads} of −0.37 eV, and they predicted that Ti_2CO_2 has application prospects in the NH_3 sensor with high selectivity and sensitivity. Our results exhibit that the adsorption strength of H_2S, NO_2, and CO_2 on MSN is comparable to that of NO_2 on InSe and NH_3 on Ti_2CO_2, which reveals that the MSN monolayer may be utilized in H_2S, NO_2, and CO_2 sensing. Moreover, the nearest distance between the adsorbed molecules and the MSN monolayer is in the range of 2.14−3.24 Å. After optimization, the bond lengths and bond angles of NO, CO, O_2, CO_2, NO_2, H_2O, H_2S, and NH_3 slightly changed compared to those of the free gas molecules (see Table S2). The slightly changed bond lengths and angles of gas molecules after adsorption suggest the weak interaction between gas molecules and the MSN surface, indicating that the adsorption type is physisorption.

As we all know, there usually exist surface vacancies in the CVD-grown 2D materials, and the defective regions are usually chemically active and proved to enhance the interaction between the gas molecules and the substrate.[44,61,62] Qian et al.[63] reported that the surface N-defective MSN is much more stable than that of inner N vacancy and surface Si vacancy, and the d-MSN is also proved to be thermodynamically stable via the ab initio molecular dynamics simulation.[58] Based on the above results, we further investigate the adsorption behavior of small molecules on the surface of N-defective MSN in this work. Several initial adsorption structures of the d-MSN system are shown in Figures S5 and S6. The most stable adsorption structures and corresponding E_{ads} are illustrated in Figure 4 and Figure 3, respectively. The E_{ads} values of other metastable adsorption structures are summarized in Table S3. It can be clearly observed that NO and CO molecules tend to be vertically adsorbed on the surface of d-MSN with the vacancy occupied by the N or C atom. NO_2 dissociates into an O atom and a NO molecule after the full optimization in which the O atom occupies the surface N vacancy and the NO molecule located on the topsite of the Si atom adjacent to the N vacancy. The same phenomenon also occurs in the O_2 adsorption case; the two O atoms are dissociated with one O atom occupying the N vacancy and the other locating on the topsite of the Si−Si bond. Moreover, the rest of the molecules including CO_2, H_2O, H_2S, and NH_3 tend to be adsorbed in a parallel manner on the top of the Si atom adjacent to the N vacancy. From Figure 3, we can clearly observe that the E_{ads} of the molecules on d-MSN is lower than that of MSN, indicating that adsorption on d-MSN is much stronger than that on MSN. The adsorption capacity of the above molecules on d-MSN is arranged in the following order: CO_2 < H_2S < H_2O < NH_3 < CO < NO_2 < NO < O_2. In addition, we also calculated the adsorption energies of (d-)MSN systems via a more precise hybrid functional (HSE06),[64] which is shown in Figure S7. We can clearly observe that the change trend of adsorption strength of the gas molecules on the (d-)MSN surface is consistent with the PBE functional. After optimization, the bond length of NO and CO increases significantly, indicating their activation, while the bond length and angle of CO_2, H_2O, H_2S, and NH_3 slightly change compared to that of free gas molecules (see Table S2). Combining the E_{ads} and the change

https://doi.org/10.1021/acsomega.1c06860
ACS Omega 2022, 7, 8706−8716

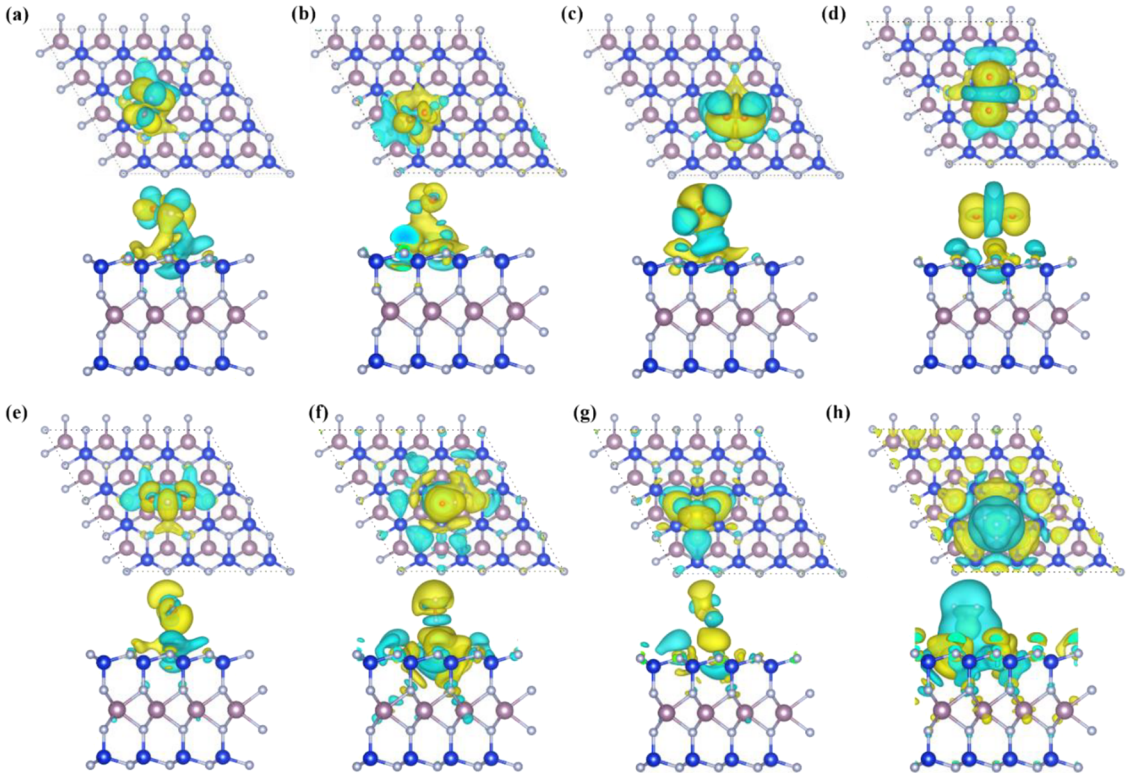

Figure 5. Calculated charge density difference of MSN adsorbing (a) NO (isovalue: 0.0001 e/Å^3), (b) CO (isovalue: 0.00005 e/Å^3), (c) O_2 (0.00002 e/Å^3), (d) CO_2 (isovalue: 0.0001 e/Å^3), (e) NO_2 (isovalue: 0.0001 e/Å^3), (f) H_2O (isovalue: 0.0001 e/Å^3), (g) H_2S (isovalue: 0.0001 e/Å^3), and (h) NH_3 (isovalue: 0.0001 e/Å^3). The electron depletion and electron accumulation are illustrated by light-blue and yellow isosurfaces, respectively.

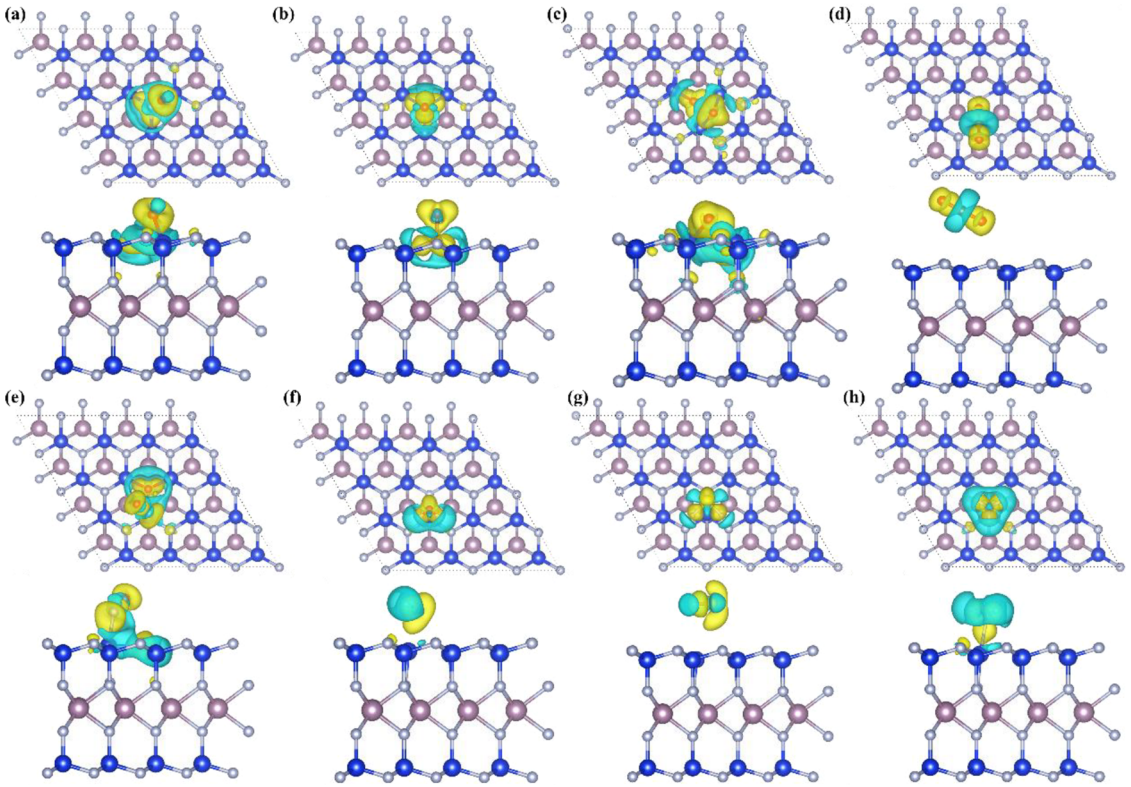

Figure 6. Calculated charge density difference of d-MSN adsorbing (a) NO, (b) CO, (c) O_2, (d) CO_2, (e) NO_2, (f) H_2O, (g) H_2S, and (h) NH_3 (isovalues: 0.005 e/Å^3).

https://doi.org/10.1021/acsomega.1c06860
ACS Omega 2022, 7, 8706−8716

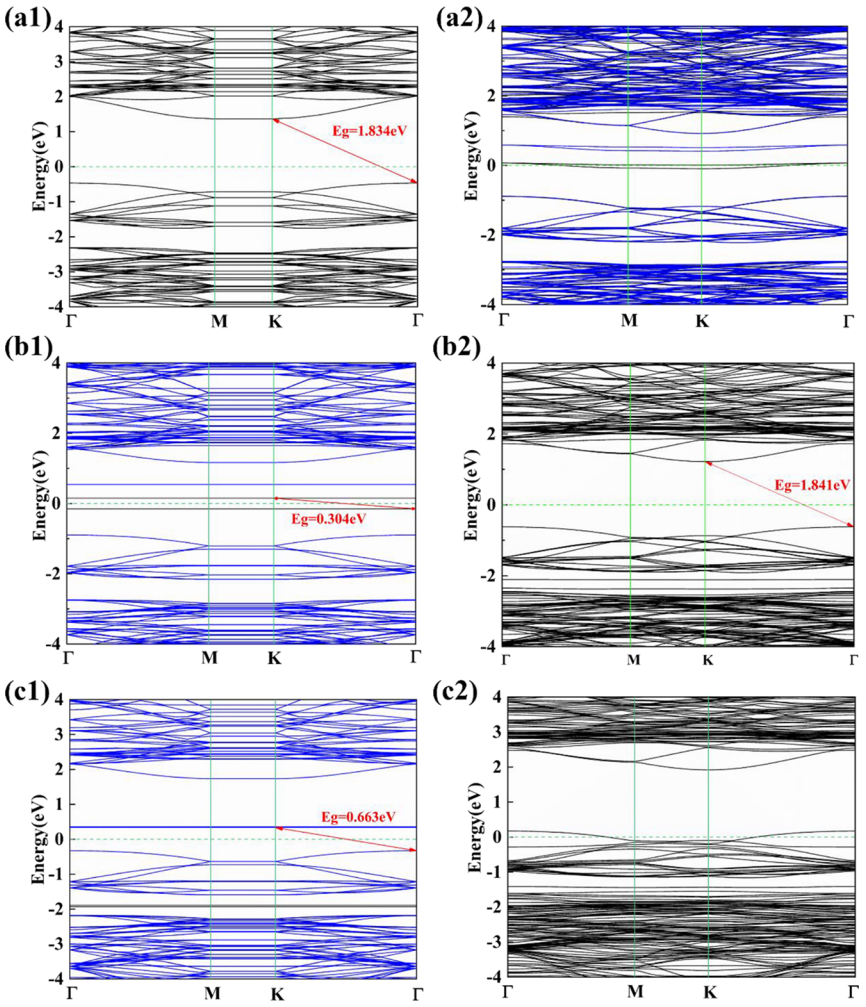

Figure 7. Band structures of (a) (d-)MSN adsorbing (b) NO and (c) O_2. The spin-up and spin-down bands are shown in black and blue lines, respectively. The Fermi level is set to zero. (*1) and (*2) represent the MSN and d-MSN adsorption systems, respectively.

of structural parameters, we find that some gas molecules (NO, CO, O_2, and NO_2) favor chemisorption on the d-MSN surface, while the rest of gas molecules tend to be adsorbed in the form of physisorption. Interestingly, the calculated E_{ads} values of NO (−5.42 eV) and CO (−2.60 eV) on the d-MSN are more negative than those of the other 2D materials, such as defective graphene (−3.04 eV for NO and −2.33 eV for CO),[65] defective Fe_3GeTe_2 (−3.71 eV for NO and −2.44 eV for CO),[61] and defective blue phosphorus (−1.12 eV for NO).[44] These results show that the d-MSN has better affinity to NO and CO than the above 2D defective materials, which may be beneficial for NO and CO catalytic reaction. Furthermore, the enhanced adsorption strength of CO_2, H_2O, H_2S, and NH_3 on d-MSN might make it have better gas sensing capacity.

3.3. Charge Transfer and Electronic Structures. To gain deeper insight into the adsorption interactions between various gas molecules and the (d-)MSN surface, the charge density difference (CDD) is calculated and illustrated in Figures 5 and 6. The electron depletion and electron accumulation are shown in light-blue and yellow isosurfaces, respectively. As we can see from Figure 5, all the gas molecules (except NH_3) are mostly surrounded by electron-accumulation regions accompanied by a small fraction of electron-depletion regions. Moreover, there exist electron-accumulation regions near the interface between most gas molecules (including CO, CO_2, NO_2, and H_2S) and the MSN surface. These results demonstrate that these molecules except NH_3 serve as electron acceptors in corresponding adsorption systems. In the case of NH_3 adsorption, the charges mainly deplete around the NH_3 molecule, whereas most charges accumulate on the N atoms of the MSN surface. This phenomenon suggests that the NH_3 molecule donates electrons to the MSN monolayer, acting as an electron donor. The above analysis of charge transfer between gas molecules and MSN is consistent with the Bader charge analysis, which is shown in Figure 2. We can easily observe that NO, NO_2, and H_2O act as strong acceptors, receiving the greatest number of electrons, while NH_3 acts as an effective donor, donating electrons to the substrate. The weak charge transfer between gas molecules and the MSN surface also proves that the adsorption is physisorption.

As for d-MSN adsorption systems, the CDD is calculated and plotted in Figure 6. In most adsorption cases, such as CO, NO, O_2, and NO_2 adsorption cases, electrons accumulate near the gas molecules and Si−X bond (X denotes the atoms of the gas molecules), while electrons deplete in the Si atoms around the N vacancy, indicating that these gas molecules act as electron acceptors. However, the remaining adsorption systems have less charge transfer between gas molecules and d-MSN, and the charge mainly transfers within gas molecules. The Bader charge analysis is also applied to investigate the

https://doi.org/10.1021/acsomega.1c06860
ACS Omega 2022, 7, 8706−8716

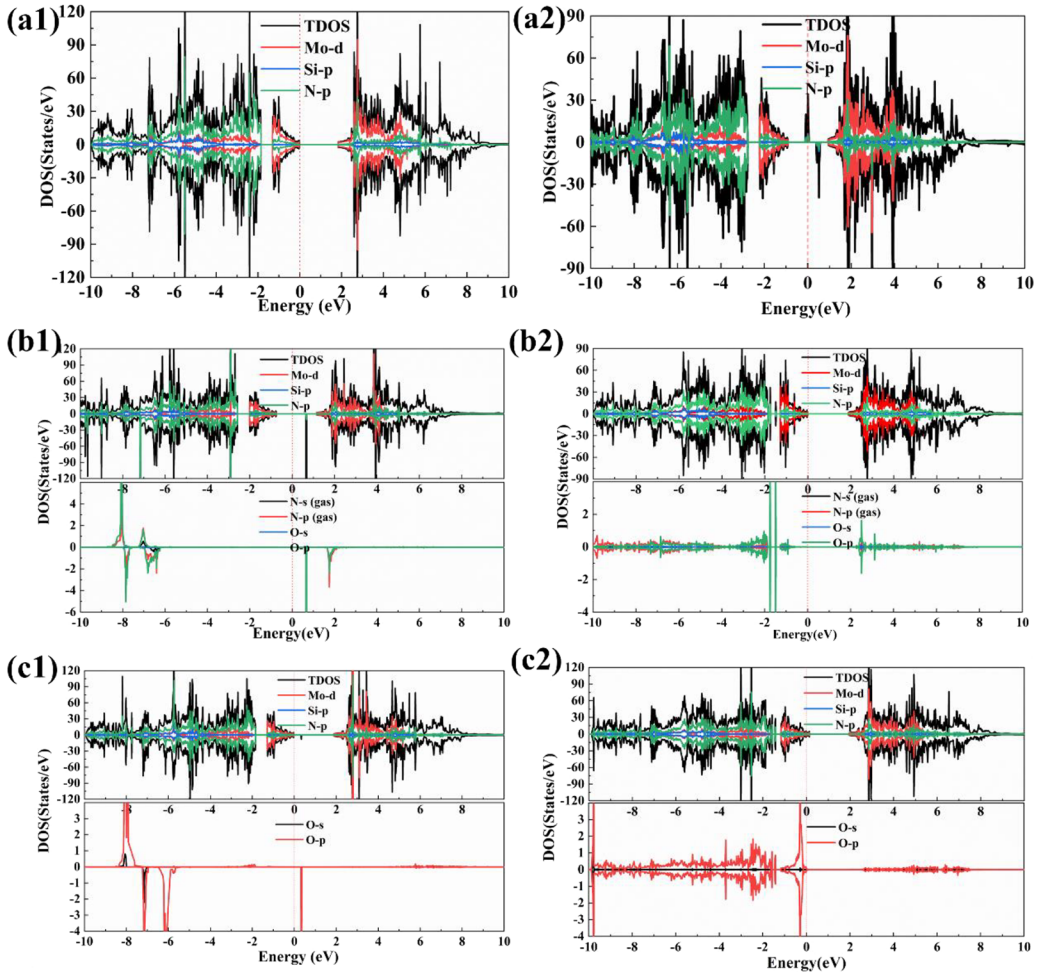

Figure 8. Calculated DOS and local DOS (LDOS) of (a) (d-)MSN adsorbing (b) NO and (c) O_2. The Fermi level is set to zero. (*1) and (*2) represent the MSN and d-MSN adsorption systems, respectively. The Fermi level is set to zero.

interaction between the d-MSN and gas molecules. Based on Bader charge values, the calculated charge transfer values between these molecules and d-MSN are +2.305*e* (NO), +2.040*e* (CO), +3.081*e* (O_2), +0.015*e* (CO_2), +2.346*e* (NO_2), −0.018*e* (H_2O), −0.050*e* (H_2S), and +0.070*e* (NH_3) (the "+" denotes that the charge is transferred from d-MSN to gas molecules and vice versa). The calculated Bader charge results are in good agreement with the above analysis of CDD. Compared with the pristine MSN, the amount of charge transfer is significantly increased in most adsorption systems. According to the lower E_{ads} and more obvious charge transfer, we believe that the d-MSN has a strong bonding capacity to the gas molecules compared to MSN.

The electronic structures of the adsorption systems are also calculated to analyze the interaction mechanism between gas molecules and the substrate and the influence of gas molecule adsorption on the electronic properties of the MSN monolayer. The band structure and DOS (including LDOS) of MSN, d-MSN, and NO and O_2 adsorption systems are depicted in Figures 7 and 8, while the rest of adsorption systems are shown in Figures S7 and S8. In MSN adsorption systems, the band gap of the closed-shell molecule adsorption systems (CO, CO_2, H_2O, H_2S, and NH_3) increases to ∼2 eV, while the band gaps of MSN decrease to 0.304 eV (NO), 0.663 eV (O_2), and 0.242 eV (NO_2) after the adsorption of open-shell molecules, which is caused by the new in-gap states (see Figure 7b1,c1). The introduction of N vacancy on the MSN surface would give rise to spin-up and spin-down bands above and below the Fermi level, leading to the decrease in band gap, thus improving the electrical conductivity of the MSN monolayer. However, for NO@d-MSN (d-MSN adsorbs NO), the newly generated in-gap energy bands disappear and the band gap increases, while in O_2@d-MSN, the VBM moves up to the Fermi level.

As shown in Figure 8, we observe that the overall trend of the DOS plots of the adsorption systems is similar to that of the MSN monolayer, that is, the regions around the Fermi level are mainly contributed by Mo 4d and N 2p orbitals as well as their hybridization. The newly generated energy bands near the Fermi level in d-MSN are mainly composed of N 2p orbitals, leading to the decrease in band gap and the increase in electrical conductivity. Therefore, we believe that the d-MSN may have a high charge transfer efficiency than MSN, which makes it more suitable as a catalyst to accelerate the reaction. The NO and O_2 adsorption cases are taken as a representative to analyze the difference in electronic structures of (d-)MSN. For the NO@MSN (MSN adsorbs NO) adsorption system, there only exist some orbital hybridizations between O 2p and N 2p states of NO and TDOS of the adsorption system. However, in the NO@d-MSN adsorption system, the strong orbital hybridizations between O 2p and N 2p states of NO and the TDOS of the adsorption system occur, demonstrating that more electronic states get involved in the interaction

https://doi.org/10.1021/acsomega.1c06860
ACS Omega 2022, 7, 8706−8716

between the gas molecules and (d-)MSN substrates;[66] thus, d-MSN has a strong bonding ability to NO than MSN. Similarly, the same phenomenon occurred in O_2@(d-)MSN systems, and the greater intense orbital hybridization level is observed in O_2@d-MSN than in NO@d-MSN, indicating the stronger adsorption strength between O_2 and d-MSN, which is in good agreement with the calculated result of E_{ads} (E_{ads} (O_2@d-MSN) > E_{ads} (NO@d-MSN)). In general, the electronic structures of MSN may change after the adsorption of reactants and the changed electronic properties would affect its optical properties and electrical conductivity,[34,42] which might be conducive to gas sensing and catalytic reactions.

3.4. Possible Applications of (d-)MSN. Based on the adsorption behavior of NO, CO, O_2, CO_2, NO_2, H_2O, H_2S, and NH_3 molecules on the (d-)MSN monolayer mentioned above, the potential applications of the (d-)MSN monolayer are discussed in this part. The adsorption of reactants on the catalyst surface, as the prerequisite for subsequent processes of various reactions such as oxygen and carbon monoxide reduction reactions (ORR and CORR, respectively), determines whether the reactants can be activated.[67,68] For example, the adsorption capacity for CO and NO of d-MSN is comparable to or even better than those of Fe-anchored graphene[66] and Ga-doped Pt/CeO_2,[69] which was proved to be an excellent catalyst for the conversion and removal of CO and NO. So, we believe that the d-MSN might be a good candidate for NO and CO reduction.

Next, we focus on the potential application of the (d-)MSN monolayer as a gas sensor for the detection and monitoring of specific gas molecules. Previous relevant studies have shown that the sensitivity and reusability are the most important standards for a good gas senor.[27,33,70] Herein, the changes in the electrical conductivity of the (d-)MSN monolayer before and after gas molecule adsorption are utilized to assess the sensitivity of a gas sensor, which is described as:[27,33,71]

$$\sigma \propto \exp\left(\frac{-E_g}{2kT}\right) \tag{3}$$

where σ and E_g are the electrical conductivity and band gap of the MSN monolayer adsorbing different gas molecules, respectively, and k and T are the Boltzmann constant and the temperature, respectively. Herein, the k and T are 8.62×10^{-5} eV/K and 300 K, respectively. In general, the greater the change of electrical conductivity of the materials after gas adsorption, the better the sensitivity of gas sensors.[70,72] Based on the obtained band gap value and the above formula, we can easily observe that the electrical conductivity of MSN has been greatly changed after NO, O_2, and NO_2 adsorption (see Table S4). As for d-MSN adsorption systems, the electrical conductivity of d-MSN is sensitive to most of the above gas molecules except CO and O_2. Therefore, we can see that the MSN-based gas sensor has higher sensitivity to NO, NO_2, and O_2 sensing than other gas molecules, while the d-MSN-based gas sensor has good sensitivity to most of the above gas molecules. As we all know, the stronger the adsorption capacity of gas molecules on the (d-)MSN monolayer, the more difficult it is for them to desorb from the (d-)MSN monolayer surface, which may have a severe influence on the reusability of gas sensors. Therefore, a short recovery time is another prerequisite of a good gas sensor. The recovery time (τ) of adsorption systems is evaluated according to the transition state theory and shown in the following equation:[73]

$$\tau = {\nu_0}^{-1} \exp\left(\frac{-E_{ads}}{kT}\right) \tag{4}$$

where ν_0, E_{ads}, k, and T represent the attempt frequency, adsorption energy, Boltzmann constant, and temperature, respectively. Herein, for the sake of comparison, the attempt frequency of all the gas molecules is set to the same value as the NO_2 molecule ($\nu_0 = 10^{12}$/s).[73] The recovery times of MSN adsorbing NO, CO, O_2, CO_2, NO_2, H_2O, H_2S, and NH_3 are 1.81×10^{-9}, 2.30×10^{-10}, 9.22×10^{-11}, 2.77×10^{-9}, 2.88×10^{-9}, 1.23×10^{-9}, 4.08×10^{-9}, and 9.38×10^{-10} s, respectively. It is easy to observe that the adsorption strength of the above gas molecules on MSN is so weak that MSN cannot be utilized for gas sensing and monitoring. As for d-MSN adsorption systems, the O_2 and NO_2 adsorption systems are not considered due to their dissociation after adsorption, and the recovery times of d-MSN adsorbing NO, CO, CO_2, H_2O, H_2S, and NH_3 are 1.02×10^{79} s, 4.28×10^{31} s, 0.37 ms, 6.51 s, 0.16 s, and 5.64×10^5 s, respectively. Our results show that NO, CO, and NH_3 on d-MSN have relatively long recovery times, but the recovery time of CO_2 on d-MSN is much shorter, which is not suitable to be used for gas detection. However, the adsorption energy of H_2O and H_2S on d-MSN is moderate, which matches short recovery times of 6.51 and 0.16 s, respectively, and is appropriate for H_2O and H_2S detection. Based on the analysis of adsorption energies, adsorption structures, charge transfer, and the changes of electronic properties, the d-MSN exhibits bright application prospects in H_2O and H_2S gas sensors with high sensitivity and reusability.

To explore the effect of gas coverage on reusable gas sensors, we introduced other H_2O and H_2S molecules to the original adsorption structures, respectively. The fully optimized structures are shown in Figure S9, in which both molecules are located in the vicinity of the N vacancy. Moreover, we also calculated the effect of gas coverage on the band gap of the H_2O and H_2S adsorption systems (see Figure S10). We see that the band gaps of the double molecule adsorption systems are the same as single molecule ones, indicating that the effect of gas coverage has no effect on the band gap, and thus, it does not affect the sensitivity of the sensor.

4. CONCLUSIONS

In this work, the adsorption behavior of NO, CO, O_2, CO_2, NO_2, H_2O, H_2S, and NH_3 on the (d-)MSN monolayer was systematically investigated, focusing on the adsorption structures, charge transfer, the changes of electronic structures, and potential application of the (d-)MSN monolayer. Based on the results of adsorption energies, all the adsorption configurations are thermodynamically favorable and tend to be physisorbed on the MSN surface with small charge transfer. However, the electronic properties of NO, O_2, and NO_2 adsorption configurations are dramatically modified due to the newly introduced in-gap states. However, the introduction of N vacancy on MSN would obviously affect the interaction between gas molecules and the substrate, especially in NO_2 and O_2 adsorption systems. Furthermore, the adsorption type of NO and CO changes from physisorption to chemisorption, which may be used as catalysts for NO and CO reduction. Compared with the MSN adsorption systems, the d-MSN has moderate adsorption strength for H_2O and H_2S, thus possessing quite broad application prospects in highly sensitive and reusable gas sensors. This work provides a vital theoretical

https://doi.org/10.1021/acsomega.1c06860
ACS Omega 2022, 7, 8706−8716

reference of the 2D MA_2Z_4 family in the field of gas sensors, catalysts, and toxic gas disposal.

■ ASSOCIATED CONTENT

Supporting Information

The Supporting Information is available free of charge at https://pubs.acs.org/doi/10.1021/acsomega.1c06860.

Initial adsorption configurations of gas molecules on (d-)MSN; adsorption energies, band structures, DOS, electrical conductivity, and recovery time of adsorption systems; atomic structures and band structures of bimolecular adsorption systems (PDF)

■ AUTHOR INFORMATION

Corresponding Author

Zuju Ma − *School of Environmental and Materials Engineering, Yantai University, Yantai 264005, PR China;* orcid.org/0000-0001-5687-862X; Email: zjma@outlook.com

Authors

Chengwei Xiao − *School of Environmental and Materials Engineering, Yantai University, Yantai 264005, PR China*

Rongjian Sa − *Institute of Oceanography, Ocean College, Minjiang University, Fuzhou 350108, China;* orcid.org/0000-0002-8515-2438

Zhitao Cui − *School of Environmental and Materials Engineering, Yantai University, Yantai 264005, PR China; School of Materials Science and Engineering, Anhui University of Technology, Maanshan 243002, China*

Shuaishuai Gao − *School of Environmental and Materials Engineering, Yantai University, Yantai 264005, PR China*

Wei Du − *School of Environmental and Materials Engineering, Yantai University, Yantai 264005, PR China*

Xueqin Sun − *School of Environmental and Materials Engineering, Yantai University, Yantai 264005, PR China*

Qiao-hong Li − *State Key Laboratory of Structural Chemistry, Fujian Institute of Research on the Structure of Matter, Chinese Academy of Sciences, Fuzhou 350002, China;* orcid.org/0000-0001-9286-3580

Complete contact information is available at: https://pubs.acs.org/10.1021/acsomega.1c06860

Notes

The authors declare no competing financial interest.

■ ACKNOWLEDGMENTS

This work was supported by the National Science Foundation of China (nos. 21771182 and 21501177) and the Open Project Program of Structural Chemistry, Fujian Institute of Research on the Structure of Matter, Chinese Academy of Sciences. The authors also gratefully acknowledge the Supercomputing Center in Minjiang University for providing the computing resources. We also gratefully acknowledge HZWTECH for providing computation facilities.

■ REFERENCES

(1) Novoselov, K. S.; Geim, A. K.; Morozov, S. V.; Jiang, D.; Zhang, Y.; Dubonos, S. V.; Grigorieva, I. V.; Firsov, A. A. Electric field effect in atomically thin carbon films. *Science* **2004**, *306*, 666−669.

(2) Castro Neto, A. H.; Guinea, F.; Peres, N. M. R.; Novoselov, K. S.; Geim, A. K. The electronic properties of graphene. *Rev. Mod. Phys.* **2009**, *81*, 109−162.

(3) Hu, W.; Xia, N.; Wu, X.; Li, Z.; Yang, J. Silicene as a highly sensitive molecule sensor for NH_3, NO and NO_2. *Phys. Chem. Chem. Phys.* **2014**, *16*, 6957−6962.

(4) Prasongkit, J.; Amorim, R. G.; Chakraborty, S.; Ahuja, R.; Scheicher, R. H.; Amornkitbamrung, V. Highly Sensitive and Selective Gas Detection Based on Silicene. *J. Phys. Chem. C* **2015**, *119*, 16934−16940.

(5) Vogt, P.; De Padova, P.; Quaresima, C.; Avila, J.; Frantzeskakis, E.; Asensio, M. C.; Resta, A.; Ealet, B.; Le Lay, G. Silicene: Compelling Experimental Evidence for Graphenelike Two-Dimensional Silicon. *Phys. Rev. Lett.* **2012**, *108*, 155501.

(6) Chandiramouli, R.; Srivastava, A.; Nagarajan, V. NO adsorption studies on silicene nanosheet: DFT investigation. *Appl. Surf. Sci.* **2015**, *351*, 662−672.

(7) Cui, S.; Pu, H.; Wells, S. A.; Wen, Z.; Mao, S.; Chang, J.; Hersam, M. C.; Chen, J. Ultrahigh sensitivity and layer-dependent sensing performance of phosphorene-based gas sensors. *Nat. Commun.* **2015**, *6*, 8632.

(8) Kou, L.; Frauenheim, T.; Chen, C. Phosphorene as a Superior Gas Sensor: Selective Adsorption and Distinct *I*−*V* Response. *J. Phys. Chem. Lett.* **2014**, *5*, 2675−2681.

(9) Elías, A. L.; Perea-López, N.; Castro-Beltrán, A.; Berkdemir, A.; Lv, R.; Feng, S.; Long, A. D.; Hayashi, T.; Kim, Y. A.; Endo, M.; Gutiérrez, H. R.; Pradhan, N. R.; Balicas, L.; Mallouk, T. E.; López-Urías, F.; Terrones, H.; Terrones, M. Controlled Synthesis and Transfer of Large-Area WS_2 Sheets: From Single Layer to Few Layers. *ACS Nano* **2013**, *7*, 5235−5242.

(10) Chhowalla, M.; Shin, H. S.; Eda, G.; Li, L.-J.; Loh, K. P.; Zhang, H. The chemistry of two-dimensional layered transition metal dichalcogenide nanosheets. *Nat. Chem.* **2013**, *5*, 263−275.

(11) Panigrahi, P.; Hussain, T.; Karton, A.; Ahuja, R. Elemental Substitution of Two-Dimensional Transition Metal Dichalcogenides ($MoSe_2$ and $MoTe_2$): Implications for Enhanced Gas Sensing. *ACS Sens.* **2019**, *4*, 2646−2653.

(12) Zhu, J.; Zhang, H.; Tong, Y.; Zhao, L.; Zhang, Y.; Qiu, Y.; Lin, X. First-principles investigations of metal (V, Nb, Ta)-doped monolayer MoS_2: Structural stability, electronic properties and adsorption of gas molecules. *Appl. Surf. Sci.* **2017**, *419*, 522−530.

(13) Zhao, S.; Xue, J.; Kang, W. Gas adsorption on MoS_2 monolayer from first-principles calculations. *Chem. Phys. Lett.* **2014**, *595-596*, 35−42.

(14) Mananghaya, M. R. Adsorption of CO and desorption of CO_2 interacting with Pt (111) surface: a combined density functional theory and Kinetic Monte Carlo simulation. *Adsorption* **2020**, *26*, 461−469.

(15) Mananghaya, M. Transport properties of Ag decorated zigzag graphene nanoribbons as a function of temperature: a density functional based tight binding molecular dynamics study. *Adsorption* **2019**, *25*, 1655−1662.

(16) Mananghaya, M. R.; Santos, G. N.; Yu, D. Small transition metal cluster adsorbed on graphene and graphene nanoribbons: A density functional based tight binding molecular dynamics study. *Org. Electron.* **2018**, *63*, 355−361.

(17) Pumera, M. Graphene-based nanomaterials for energy storage. *Energy Environ. Sci.* **2011**, *4*, 668−674.

(18) Yang, X.; Cheng, C.; Wang, Y.; Qiu, L.; Li, D. Liquid-Mediated Dense Integration of Graphene Materials for Compact Capacitive Energy Storage. *Science* **2013**, *341*, 534−537.

(19) Cui, Z.; Du, W.; Xiao, C.; Li, Q.; Sa, R.; Sun, C.; Ma, Z. Enhancing hydrogen evolution of MoS_2 basal planes by combining single-boron catalyst and compressive strain. *Front Phys.* **2020**, *15*, 63502.

(20) Ma, Z.; Cui, Z.; Lv, Y.; Sa, R.; Wu, K.; Li, Q. Three-in-One: Opened Charge-transfer channel, positively shifted oxidation potential, and enhanced visible light response of g-C_3N_4 photocatalyst

through K and S Co-doping. *Int. J. Hydrogen Energy* **2020**, *45*, 4534−4544.
(21) Ma, Z.; Cui, Z.; Xiao, C.; Dai, W.; Lv, Y.; Li, Q.; Sa, R. Theoretical screening of efficient single-atom catalysts for nitrogen fixation based on a defective BN monolayer. *Nanoscale* **2020**, *12*, 1541−1550.
(22) Xiao, C.; Sa, R.; Ma, Z.; Cui, Z.; Du, W.; Sun, X.; Li, Q.; Deng, H. High-throughput screening of transition metal single-atom catalyst anchored on Janus MoSSe basal plane for hydrogen evolution reaction. *Int. J. Hydrogen Energy* **2021**, *46*, 10337−10345.
(23) Liu, Z.; Wang, H.; Sun, J.; Sun, R.; Wang, Z. F.; Yang, J. Penta-Pt_2N_4: an ideal two-dimensional material for nanoelectronics. *Nanoscale* **2018**, *10*, 16169−16177.
(24) Fiori, G.; Bonaccorso, F.; Iannaccone, G.; Palacios, T.; Neumaier, D.; Seabaugh, A.; Banerjee, S. K.; Colombo, L. Electronics based on two-dimensional materials. *Nat. Nanotechnol.* **2014**, *9*, 768−779.
(25) Qin, H.; Feng, C.; Luan, X.; Yang, D. First-principles investigation of adsorption behaviors of small molecules on penta-graphene. *Nanoscale Res. Lett.* **2018**, *13*, 264.
(26) Tian, B.; Huang, T.; Guo, J.; Shu, H.; Wang, Y.; Dai, J. Gas adsorption on the pristine monolayer GeP_3: A first-principles calculation. *Vacuum* **2019**, *164*, 181−185.
(27) Yong, Y.; Cui, H.; Zhou, Q.; Su, X.; Kuang, Y.; Li, X. C_2N monolayer as NH_3 and NO sensors: A DFT study. *Appl. Surf. Sci.* **2019**, *487*, 488−495.
(28) Hong, Y.-L.; Liu, Z.; Wang, L.; Zhou, T.; Ma, W.; Xu, C.; Feng, S.; Chen, L.; Chen, M.-L.; Sun, D.-M.; Chen, X.-Q.; Cheng, H.-M.; Ren, W. Chemical vapor deposition of layered two-dimensional $MoSi_2N_4$ materials. *Science* **2020**, *369*, 670−674.
(29) Bafekry, A.; Faraji, M.; Hoat, D. M.; Shahrokhi, M.; Fadlallah, M. M.; Shojaei, F.; Feghhi, S. A. H.; Ghergherehchi, M.; Gogova, D. $MoSi_2N_4$ single-layer: a novel two-dimensional material with outstanding mechanical, thermal, electronic and optical properties. *J. Phys. D: Appl. Phys.* **2021**, *54*, 155303.
(30) Cai, Y.; Zhang, G.; Zhang, Y.-W. Polarity-Reversed Robust Carrier Mobility in Monolayer MoS_2 Nanoribbons. *J. Am. Chem. Soc.* **2014**, *136*, 6269−6275.
(31) Cao, L.; Zhou, G.; Wang, Q.; Ang, L. K.; Ang, Y. S. Two-dimensional van der Waals electrical contact to monolayer $MoSi_2N_4$. *Appl. Phys. Lett.* **2021**, *118*, No. 013106.
(32) Guo, X.-S.; Guo, S.-D. Tuning transport coefficients of monolayer $MoSi_2N_4$ with biaxial strain. *Chin. Phys. B* **2021**, *30*, No. 067102.
(33) Yong, Y.; Cui, H.; Zhou, Q.; Su, X.; Kuang, Y.; Li, X. Adsorption of gas molecules on a graphitic GaN sheet and its implications for molecule sensors. *RSC Adv.* **2017**, *7*, 51027−51035.
(34) Cai, Y.; Zhang, G.; Zhang, Y.-W. Charge Transfer and Functionalization of Monolayer InSe by Physisorption of Small Molecules for Gas Sensing. *J. Phys. Chem. C* **2017**, *121*, 10182−10193.
(35) Cai, Y.; Ke, Q.; Zhang, G.; Zhang, Y.-W. Energetics, Charge Transfer, and Magnetism of Small Molecules Physisorbed on Phosphorene. *J. Phys. Chem. C* **2015**, *119*, 3102−3110.
(36) Li, H.; Wu, J.; Yin, Z.; Zhang, H. Preparation and Applications of Mechanically Exfoliated Single-Layer and Multilayer MoS_2 and WSe_2 Nanosheets. *Acc. Chem. Res.* **2014**, *47*, 1067−1075.
(37) Huang, B.; Li, Z.; Liu, Z.; Zhou, G.; Hao, S.; Wu, J.; Gu, B.-L.; Duan, W. Adsorption of Gas Molecules on Graphene Nanoribbons and Its Implication for Nanoscale Molecule Sensor. *J. Phys. Chem. C* **2008**, *112*, 13442−13446.
(38) Chen, Z.; Darancet, P.; Wang, L.; Crowther, A. C.; Gao, Y.; Dean, C. R.; Taniguchi, T.; Watanabe, K.; Hone, J.; Marianetti, C. A.; Brus, L. E. Physical Adsorption and Charge Transfer of Molecular Br_2 on Graphene. *ACS Nano* **2014**, *8*, 2943−2950.
(39) Hu, T.; Gerber, I. C. Theoretical Study of the Interaction of Electron Donor and Acceptor Molecules with Graphene. *J. Phys. Chem. C* **2013**, *117*, 2411−2420.
(40) Zhou, M.; Lu, Y.-H.; Cai, Y.-Q.; Zhang, C.; Feng, Y.-P. Adsorption of gas molecules on transition metal embedded graphene: a search for high-performance graphene-based catalysts and gas sensors. *Nanotechnology* **2011**, *22*, 385502.
(41) Leenaerts, O.; Partoens, B.; Peeters, F. M. Adsorption of HO_2, NH_3, CO, NO_2, and NO on graphene: A first-principles study. *Phys. Rev. B* **2008**, *77*, 125416.
(42) Chen, X.; Tan, C.; Yang, Q.; Meng, R.; Liang, Q.; Cai, M.; Zhang, S.; Jiang, J. Ab Initio Study of the Adsorption of Small Molecules on Stanene. *J. Phys. Chem. C* **2016**, *120*, 13987−13994.
(43) Garg, P.; Choudhuri, I.; Pathak, B. Stanene based gas sensors: effect of spin−orbit coupling. *Phys. Chem. Chem. Phys.* **2017**, *19*, 31325−31334.
(44) Liu, N.; Zhou, S. Gas adsorption on monolayer blue phosphorus: implications for environmental stability and gas sensors. *Nanotechnology* **2017**, *28*, 175708.
(45) Ma, D.; Ju, W.; Tang, Y.; Chen, Y. First-principles study of the small molecule adsorption on the InSe monolayer. *Appl. Surf. Sci.* **2017**, *426*, 244−252.
(46) Yue, Q.; Shao, Z.; Chang, S.; Li, J. Adsorption of gas molecules on monolayer MoS_2 and effect of applied electric field. *Nanoscale Res. Lett.* **2013**, *8*, 425.
(47) Kou, L.; Du, A.; Chen, C.; Frauenheim, T. Strain engineering of selective chemical adsorption on monolayer MoS_2. *Nanoscale* **2014**, *6*, 5156−5161.
(48) Novoselov, K. S.; Fal'ko, V. I.; Colombo, L.; Gellert, P. R.; Schwab, M. G.; Kim, K. A roadmap for graphene. *Nature* **2012**, *490*, 192−200.
(49) Bafekry, A.; Faraji, M.; Fadlallah, M. M.; Abdolahzadeh Ziabari, A.; Bagheri Khatibani, A.; Feghhi, S. A. H.; Ghergherehchi, M.; Gogova, D. Adsorption of habitat and industry-relevant molecules on the $MoSi_2N_4$ monolayer. *Appl. Surf. Sci.* **2021**, *564*, 150326.
(50) Kresse, G.; Furthmüller, J. Efficient iterative schemes for ab initio total-energy calculations using a plane-wave basis set. *Phys. Rev. B* **1996**, *54*, 11169−11186.
(51) Kresse, G.; Furthmüller, J. Efficiency of ab-initio total energy calculations for metals and semiconductors using a plane-wave basis set. *Comput. Mater. Sci.* **1996**, *6*, 15−50.
(52) Kresse, G.; Joubert, D. From ultrasoft pseudopotentials to the projector augmented-wave method. *Phys. Rev. B* **1999**, *59*, 1758−1775.
(53) Perdew, J. P.; Chevary, J. A.; Vosko, S. H.; Jackson, K. A.; Pederson, M. R.; Singh, D. J.; Fiolhais, C. Atoms, molecules, solids, and surfaces: applications of the generalized gradient approximation for exchange and correlation. *Phys. Rev. B* **1992**, *46*, 6671−6687.
(54) Grimme, S. Accurate description of van der Waals complexes by density functional theory including empirical corrections. *J. Comput. Chem.* **2004**, *25*, 1463−1473.
(55) Cai, X. H.; Yang, Q.; Pang, Y.; Wang, M. Adsorption of CO_2, CO, NH_3, NO_2 and NO on g-C_3N_5 surface by first-principles calculations. *Appl. Surf. Sci.* **2021**, *537*, 147884.
(56) Yu, X.-f.; Li, Y.-c.; Cheng, J.-b.; Liu, Z.-b.; Li, Q.-z.; Li, W.-z.; Yang, X.; Xiao, B. Monolayer Ti_2CO_2: A Promising Candidate for NH_3 Sensor or Capturer with High Sensitivity and Selectivity. *ACS Appl. Mater. Interfaces* **2015**, *7*, 13707−13713.
(57) Momma, K.; Izumi, F. VESTA 3 for three-dimensional visualization of crystal, volumetric and morphology data. *J. Appl. Crystallogr.* **2011**, *44*, 1272−1276.
(58) Bafekry, A.; Faraji, M.; Fadlallah, M. M.; Bagheri Khatibani, A.; abdolahzadeh Ziabari, A.; Ghergherehchi, M.; Nedaei, S.; Shayesteh, S. F.; Gogova, D. Tunable electronic and magnetic properties of $MoSi_2N_4$ monolayer via vacancy defects, atomic adsorption and atomic doping. *Appl. Surf. Sci.* **2021**, *559*, 149862.
(59) Zeng, J.; Xu, L.; Yang, Y.; Luo, X.; Li, H.-J.; Xiong, S. X.; Wang, L.-L. Boosting the photocatalytic hydrogen evolution performance of monolayer C_2N coupled with $MoSi_2N_4$: density-functional theory calculations. *Phys. Chem. Chem. Phys.* **2021**, *23*, 8318−8325.
(60) Bafekry, A.; Faraji, M.; Abdollahzadeh Ziabari, A.; Fadlallah, M. M.; Nguyen, C. V.; Ghergherehchi, M.; Feghhi, S. A. H. A van der

https://doi.org/10.1021/acsomega.1c06860
ACS Omega 2022, 7, 8706−8716

Waals heterostructure of $MoS_2/MoSi_2N_4$: a first-principles study. *New J. Chem.* **2021**, *45*, 8291−8296.
(61) Cui, Z.; Xiao, C.; Lv, Y.; Li, Q.; Sa, R.; Ma, Z. Adsorption behavior of CO, CO_2, H_2, H_2O, NO, and O_2 on pristine and defective 2D monolayer ferromagnetic Fe_3GeTe_2. *Appl. Surf. Sci.* **2020**, *527*, 146894.
(62) Ma, Z.; Xiao, C.; Cui, Z.; Du, W.; Li, Q.; Sa, R.; Sun, C. Defective Fe_3GeTe_2 monolayer as a promising electrocatalyst for spontaneous nitrogen reduction reaction. *J. Mater. Chem. A* **2021**, *9*, 6945−6954.
(63) Qian, W.; Chen, Z.; Zhang, J.; Yin, L. Monolayer $MoSi_2N_{4-x}$ as promising electrocatalyst for hydrogen evolution reaction: A DFT prediction. *J. Mater. Sci. Technol.* **2022**, *99*, 215−222.
(64) Heyd, J.; Scuseria, G. E.; Ernzerhof, M. Hybrid functionals based on a screened Coulomb potential. *J. Chem. Phys.* **2003**, *118*, 8207−8215.
(65) Zhang, Y.-H.; Chen, Y.-B.; Zhou, K.-G.; Liu, C.-H.; Zeng, J.; Zhang, H.-L.; Peng, Y. Improving gas sensing properties of graphene by introducing dopants and defects: a first-principles study. *Nanotechnology* **2009**, *20*, 185504.
(66) Chen, W.; Tang, Y.; Zhang, H.; Shi, J.; Wang, Z.; Cui, Y.; Teng, D.; Li, Z.; Dai, X. Modulating the stability, electronic and reactivity properties of single-atom catalyst anchored graphene by coordination environments. *Phys. E* **2022**, *135*, 114975.
(67) Tao, H.; Fan, Q.; Ma, T.; Liu, S.; Gysling, H.; Texter, J.; Guo, F.; Sun, Z. Two-dimensional materials for energy conversion and storage. *Prog. Mater. Sci.* **2020**, *111*, 100637.
(68) Sun, Z.; Ma, T.; Tao, H.; Fan, Q.; Han, B. Fundamentals and Challenges of Electrochemical CO_2 Reduction Using Two-Dimensional Materials. *Chem* **2017**, *3*, 560−587.
(69) Feng, Y.; Wan, Q.; Xiong, H.; Zhou, S.; Chen, X.; Pereira Hernandez, X. I.; Wang, Y.; Lin, S.; Datye, A. K.; Guo, H. Correlating DFT Calculations with CO Oxidation Reactivity on Ga-Doped Pt/CeO_2 Single-Atom Catalysts. *J. Phys. Chem. C* **2018**, *122*, 22460−22468.
(70) Mehdi Aghaei, S.; Monshi, M. M.; Torres, I.; Zeidi, S. M. J.; Calizo, I. DFT study of adsorption behavior of NO, CO, NO_2, and NH_3 molecules on graphene-like BC_3: A search for highly sensitive molecular sensor. *Appl. Surf. Sci.* **2018**, *427*, 326−333.
(71) Li, S., *Semiconductor Physical Electronics*; Springer Science & BusinessMedia, 2012.
(72) Yong, Y.; Su, X.; Cui, H.; Zhou, Q.; Kuang, Y.; Li, X. Two-Dimensional Tetragonal GaN as Potential Molecule Sensors for NO and NO_2 Detection: A First-Principle Study. *ACS Omega* **2017**, *2*, 8888−8895.
(73) Peng, S.; Cho, K.; Qi, P.; Dai, H. Ab initio study of CNT NO_2 gas sensor. *Chem. Phys. Lett.* **2004**, *387*, 271−276.

https://doi.org/10.1021/acsomega.1c06860
ACS Omega 2022, 7, 8706−8716